View metadata, citation and similar papers at core.ac.uk

brought to you by CORE

provided by Elsevier - Publisher Connector

Cell, Vol. 114, 359–370, August 8, 2003, Copyright ©2003 by Cell Press

Histone H2AX: A Dosage-Dependent Suppressor of Oncogenic Translocations and Tumors

Craig H. Bassing,[1] Heikyung Suh,[1] David O. Ferguson,[1,4] Katrin F. Chua,[1] John Manis,[1] Mark Eckersdorff,[1] Megan Gleason,[1] Rodrick Bronson,[2] Charles Lee,[3] and Frederick W. Alt[1,*]

[1]Howard Hughes Medical Institute
The Children's Hospital
Department of Genetics
Harvard Medical School and
The Center for Blood Research
Boston, Massachusetts 02115

[2]Tufts University School of Veterinary Medicine
200 Westboro Road
North Grafton, Massachusetts 01536

[3]Division of Cytogenetics

[4]Department of Pathology
Brigham and Woman's Hospital
Harvard Medical School
Boston, Massachusetts 02115

Summary

We employed gene targeting to study H2AX, a histone variant phosphorylated in chromatin surrounding DNA double-strand breaks. Mice deficient for both H2AX and p53 ($H^{\Delta/\Delta}P^{-/-}$) rapidly developed immature T and B lymphomas and solid tumors. Moreover, H2AX haploinsufficiency caused genomic instability in normal cells and, on a p53-deficient background, early onset of various tumors including more mature B lymphomas. Most $H2AX^{\Delta/\Delta}p53^{-/-}$ or $H2AX^{+/\Delta}p53^{-/-}$ B lineage lymphomas harbored chromosome 12 (IgH)/15 (c-*myc*) translocations with hallmarks of either aberrant V(D)J or class switch recombination. In contrast, $H2AX^{\Delta/\Delta}p53^{-/-}$ thymic lymphomas had clonal translocations that did not involve antigen receptor loci and which likely occurred during cellular expansion. Thus, H2AX helps prevent aberrant repair of both programmed and general DNA breakage and, thereby, functions as a dosage-dependent suppressor of genomic instability and tumors in mice. Notably, *H2AX* maps to a cytogenetic region frequently altered in human cancers, possibly implicating similar functions in man.

Introduction

DNA double-strand breaks (DSBs) result from exogenous factors, stalled replication forks, or genetically programmed processes such as those that occur in developing lymphocytes. Proper DSB repair is essential for maintenance of genomic stability and tumor suppression. In mammalian cells, DSBs are repaired largely by homologous recombination (HR), which is predominant in the S and G2 cell cycle phases, and by nonhomologous end joining (NHEJ), which predominates in G1 (reviewed in Jackson, 2002). Mutation of genes encoding HR factors in mice causes increased ionizing radiation (IR) sensitivity, genomic instability, and embryonic lethality, while in humans, such mutations have been linked to cancer predisposition (reviewed in Jackson, 2002). In mice, inactivation of NHEJ genes causes IR sensitivity, genomic instability, severely impaired lymphocyte development, and dramatically increased lymphoma predisposition in the context of p53 tumor suppressor deficiency (reviewed in Bassing et al., 2002b). Oncogenic translocations, such as those frequently observed in lymphomas, may result from misrepair of both general and programmed DSBs, and their junctions can provide substantial mechanistic insight into tumor etiology (reviewed in Mills et al., 2003).

During lymphocyte development, immunoglobulin (Ig) and T cell receptor (TCR)-variable region exons are assembled by V(D)J recombination, the lymphoid-specific process in which V, D, and J gene segments liberated by RAG1/2 endonuclease-generated DSBs are joined into complete V(D)J coding exons (V genes) via NHEJ (reviewed in Bassing et al., 2002b). Bone marrow progenitor (pro)-B cells and thymic $CD4^-/CD8^-$ (DN) pro-T cells assemble IgH and TCRβ V genes, respectively. Expression of IgHμ or TCRβ chains leads to differentiation of precursor (pre)-B or $CD4^+/CD8^+$ (DP) T lineage cells in which, respectively, the majority of IgL (κ or λ) or TCRα V genes are assembled. Subsequently, expression of complete (IgH/IgL) Ig or αβ TCR leads to the generation of IgM^+ B lymphocytes and $\alpha/\beta TCR^+$ T lymphocytes that migrate to the spleen and lymph nodes. Following antigen stimulation, mature B cells can undergo class-switch recombination (CSR), which replaces the IgHμ constant region (C_μ) exons (gene) with a downstream C_H gene and results in expression of a different Ig class (e.g., IgG or IgE). CSR is initiated by activation-induced deaminase (AID), may involve DSBs, and occurs between large, highly repetitive switch (S) regions that precede each C_H gene (reviewed in Manis et al., 2002).

NHEJ-deficient mice show, at most, a modest predisposition to cancer. However, combined deficiency for NHEJ and p53 leads to rapid development of pro-B lymphomas (reviewed in Bassing et al., 2002b). In this regard, p53 monitors DSBs in the context of G1 checkpoints and signals either arrest to repair DSBs or apoptosis to eliminate cells with persistent DSBs (Vogelstein et al., 2000). Thus, NHEJ-/p53-deficient pro-B cell lymphomas are proposed to result from double mutant pro-B cells generating unresolved RAG-initiated DSBs at the IgH joining (J_H) locus on chromosome (chr) 12 during G1; these cells progress into S phase and replicate the J_H DSBs. Ultimately, such replicated DSBs can be fused to chr 15 sequences downstream of c-*myc* to generate both a der(12)t(12;15) chromosomal translocation, subsequently denoted C12;15, and a complex translocation that harbors amplified IgH and c-*myc* sequences, which is termed a complicon (Zhu et al., 2002). Complicons arise from translocations that generate a dicentric 12;15, with subsequent amplification resulting via a breakage-fusion-bridge (BFB) mechanism (Difilippantonio et al., 2002; Zhu et al., 2002).

*Correspondence: alt@enders.tch.harvard.edu

Certain evidence suggests a role for histone H2AX, a mammalian core histone H2A variant, in sensing or processing DSBs. H2AX represents, on average, about 15% of the cellular H2A pool and is randomly incorporated into nucleosomes (Rogakou et al., 1998). DSBs cause rapid H2AX phosphorylation (a form called γ-H2AX) along flanking megabase chromatin regions (Rogakou et al., 1998, 1999). H2AX contains a conserved carboxy-terminal SQE motif that is the consensus target of PI3 kinases, including DNA-PKcs, ATM, and ATR. These kinases appear to phosphorylate H2AX following IR, replication stress, and replication-associated DSBs (Brown and Baltimore, 2003; Burma et al., 2001; Furuta et al., 2003; Paull et al., 2000; Ward and Chen, 2001), which may contribute to repair of DSBs at G1, S, or G2 checkpoints. H2AX-deficient cells are IR sensitive, have increased genomic instability, and show impaired formation of IR-induced foci of DNA repair proteins such as BRCA1 and 53BP1 (Bassing et al., 2002a; Celeste et al., 2002) that colocalize with γ-H2AX foci (Paull et al., 2000; Rappold et al., 2001; Schultz et al., 2000). H2AX-deficient cells appear impaired for HR (Bassing et al., 2002a; Celeste et al., 2002) but support normal NHEJ-dependent V(D)J recombination on extrachromosomal substrates (Bassing et al., 2002a). In *S. cerevisiae*, there is only one form of H2A, and it contains an SQE motif; phosphorylation of this motif is required for efficient DSB repair by NHEJ, but not HR (Downs et al., 2000).

H2AX-deficient mice are small, and males are sterile (Celeste et al., 2002). In the latter context, the Spo11-transesterase initiates meiotic DSBs that induce formation of γ-H2AX foci (Mahadevaiah et al., 2001). However, male sterility is thought to occur because Spo11-independent γ-H2AX foci, which cover the X-Y synaptic body, are required for meiotic sex chromosome pairing and inactivation (Celeste et al., 2002; Fernandez-Capetillo et al., 2003; Mahadevaiah et al., 2001). In wild-type mice, RAG-dependent γ-H2AX foci occur in the vicinity of the TCRα locus during V(D)J recombination (Chen et al., 2000). However, although H2AX-deficient mice exhibit reduced lymphocyte numbers (Celeste et al., 2002), there has been no direct evidence linking H2AX to V(D)J recombination. Foci of γ-H2AX also form at the IgH locus during CSR in activated B cells (Petersen et al., 2001), and CSR is impaired in H2AX-deficient mice (Celeste et al., 2002; Petersen et al., 2001). Conceivably, localization of γ-H2AX foci to Spo11- and RAG1/2-initiated DSBs or to putative AID-initiated DSBs during CSR may function to suppress aberrant recombination by activating efficient damage responses or repair processes.

Given that H2AX suppresses genomic instability in murine cells, it is notable that human *H2AX* (*H2AFX*) maps to a cytogenetic region (11q23) that is altered in a large number of human cancers (see Supplemental Table S1 online at http://www.cell.com/cgi/content/full/114/3/359/DC1). Therefore, we sought to determine whether H2AX functions as a tumor suppressor in mice.

Results

H2AX-Deficient Mice Exhibit a Modest Predisposition to T Cell Lymphomas

We generated H2AX-deficient ($H2AX^{\Delta/\Delta}$) mice from mutant ES cells in which one copy of *H2AX* coding sequences was "cleanly" deleted via the *loxP*/Cre method (Bassing et al., 2002a). These mice differ from another H2AX-deficient strain in which a drug-resistance marker replaced *H2AX* (Celeste et al., 2002), but appear similar with respect to published aspects of phenotype including smaller size, reduced lymphocyte numbers, and impaired CSR (data not shown). To determine whether H2AX-deficiency resulted in increased cancer predisposition, we followed cohorts of 26 $H2AX^{\Delta/\Delta}$, 12 $H2AX^{+/\Delta}$, and 21 $H2AX^{+/+}$ mice for about 7 months. During this time, one $H2AX^{+/\Delta}$ mouse developed a tumor (a teratoma), whereas three $H2AX^{\Delta/\Delta}$ mice succumbed to aggressive $CD4^{+}/CD8^{+}$ thymic lymphomas with an average mortality of 170 days (Supplemental Table S2). A single $H2AX^{\Delta/\Delta}$ thymic lymphoma analyzed by spectral karyotyping (SKY) harbored a clonal C14;16 translocation (Figure 2D; Supplemental Table S3). As ATM-deficient thymic lymphomas arise with a similar latency and routinely exhibit chr 14 (TCRα/δ locus) translocations (Liyanage et al., 2000), this finding is consistent with H2AX functioning in ATM-mediated surveillance of TCRα V(D)J recombination. We conclude that H2AX-deficiency causes only a modest predisposition to lymphoma.

$H2AX^{\Delta/\Delta}p53^{-/-}$ and $H2AX^{+/\Delta}p53^{-/-}$ Mice Exhibit Dramatic Predisposition to Lymphomas and Other Cancers

To test potential cooperation between p53 and H2AX in tumor suppression, we bred $H2AX^{+/\Delta}$ mice with $p53^{+/-}$ mice and then bred offspring to generate cohorts of $H2AX^{+/+}p53^{+/+}$ ($H^{+/+}P^{+/+}$), $H2AX^{+/\Delta}p53^{+/+}$ ($H^{+/\Delta}P^{+/+}$), $H2AX^{\Delta/\Delta}p53^{+/+}$ ($H^{\Delta/\Delta}P^{+/+}$), $H2AX^{+/+}p53^{-/-}$ ($H^{+/+}P^{-/-}$), $H2AX^{+/\Delta}p53^{-/-}$ ($H^{+/\Delta}P^{-/-}$), and $H2AX^{\Delta/\Delta}p53^{-/-}$ ($H^{\Delta/\Delta}P^{-/-}$) mice. All genotypes were born near expected Mendelian frequencies (Figure 1A), indicating p53 deficiency did not affect early viability of H2AX-deficient mice. In addition, all genotypes exhibited grossly normal lymphocyte development (Supplemental Figure S1), consistent with lack of a major impairment in V(D)J recombination. In this context, most DJ_H junctions were normal in $H^{\Delta/\Delta}P^{-/-}$ splenocytes, although some contained large deletions reminiscent of those found in NHEJ-deficient lymphocytes and occasionally observed in normal B cells (Supplemental Table S4; Nottenburg et al., 1987). We followed cohorts of 21 $H^{+/+}P^{-/-}$, 29 $H^{+/\Delta}P^{-/-}$, 17 $H^{\Delta/\Delta}P^{-/-}$, and 23 $H^{\Delta/\Delta}P^{+/+}$ mice for 21 weeks. None of the $H^{\Delta/\Delta}P^{+/+}$ mice developed cancer by 21 weeks (Figure 1B). Older p53-deficient mice develop thymic lymphomas and, less frequently, other tumors with an average survival of 4–6 months, depending on the genetic background (Donehower et al., 1992; Harvey et al., 1993; Jacks et al., 1994). In this regard, 5 of 21 cohort $H^{+/+}P^{-/-}$ mice succumbed to thymic lymphoma and one to a sarcoma by 21 weeks (Figure 1B, Table 1).

$H^{\Delta/\Delta}P^{-/-}$ mice had significantly shorter lifespans than other genotypes, becoming moribund with lymphomas as early as 6 weeks, with 50% mortality by 10 weeks, and the majority succumbing to lymphoma by 13 weeks (Figure 1B, Table 1). Of 17 cohort $H^{\Delta/\Delta}P^{-/-}$ mice, 12 developed aggressive thymic lymphomas, most of which were at the DP or SP stage (Table 1; Supplemental Table S3; data not shown). Three cohort $H^{\Delta/\Delta}P^{-/-}$ mice (numbers 590, 698, and 888) succumbed to widely dis-

A

Genotype	$H^{+/+}P^{+/+}$	$H^{+/\Delta}P^{+/+}$	$H^{\Delta/\Delta}P^{+/+}$	$H^{+/\Delta}P^{-/-}$	$H^{+/+}P^{-/-}$	$H^{\Delta/\Delta}P^{-/-}$
Expected	27	55	27	55	27	27
Actual	35	46	25	49	33	24

B

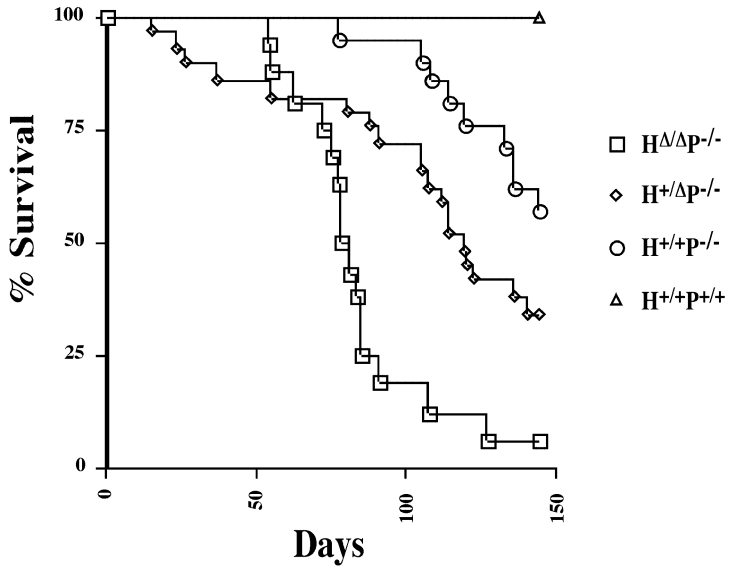

Figure 1. Effects of p53 Deficiency on Survival of $H^{\Delta/\Delta}$ and $H^{+/\Delta}$ Mice

(A) p53 deficiency does not affect early viability of H2AX-deficient mice. Shown is the expected and actual number of relevant offspring from $H^{+/\Delta}p53^{+/-}$ crosses.

(B) Kapplan-Meier curve representing the percent survival of $H^{+/+}P^{+/+}$ (n = 9), $H^{+/+}P^{-/-}$ (n = 21), $H^{+/\Delta}P^{-/-}$ (n = 29), and $H^{\Delta/\Delta}P^{-/-}$ (n = 17) cohort mice versus age in days.

seminated $B220^{+}/IgM^{-}$ B lineage lymphomas (Table 1; Supplemental Table S5), a malignancy not common in p53-deficient mice. In addition, an $H^{\Delta/\Delta}P^{-/-}$ mouse too young to be included on the cohort also developed a $B220^{+}/IgM^{-}$ B lineage lymphoma (Supplemental Tables S2 and S5). Several $H^{\Delta/\Delta}P^{-/-}$ cohort mice developed multiple cancers, including a thymic lymphoma and a pro-B cell lymphoma in #698; a thymic lymphoma, a sarcoma, and a colon adenocarcinoma in #618; an apparent (see below) pro-B cell lymphoma and a sarcoma in #888; and a thymic lymphoma and a sarcoma in #162 (Table 1; Supplemental Figure S2). Therefore, H2AX-deficiency dramatically accelerates onset of lymphomas and other cancers on a p53-deficient background.

$H^{+/\Delta}P^{-/-}$ mice also had shorter lifespans and increased cancer incidence compared to $H^{+/+}P^{-/-}$ mice (Figure 1B). Notably, a significant percentage of $H^{+/\Delta}P^{-/-}$ mice developed teratomas or lymphomas very early, with over 50% mortality by 17 weeks (Table 1; Figure 1B; Supplemental Figure S3). Three of 29 $H^{+/\Delta}P^{-/-}$ cohort mice developed B lineage lymphomas, including an $Ig\mu^{+}/IgL^{-}$ pre-B cell lymphoma, an IgM^{-} B lineage lymphoma, and an $IgG1^{+}/IgL^{+}$ mature B cell lymphoma; seven others developed thymic lymphomas (Table 1). Three slightly older $H^{+/\Delta}P^{-/-}$ mice also developed B lineage lymphomas (Supplemental Tables S2 and S5). In addition, four $H^{+/\Delta}P^{-/-}$ cohort mice developed sarcomas, including one with lung metastases, while three others developed teratomas (Table 1; Supplemental Figure S3). SKY analysis of two $H^{+/\Delta}P^{-/-}$ teratomas revealed dramatic aneuploidy, with one containing four distinct chromosomal translocations potentially implicating reduced H2AX levels (Supplemental Table S6). However, as male germ cell tumors occasionally arise

Table 1. Tumors that Developed in Cohort Mice

	$H^{\Delta/\Delta}P^{+/+}$	$H^{+/+}P^{-/-}$	$H^{+/\Delta}P^{-/-}$	$H^{\Delta/\Delta}P^{-/-}$
Number of mice	23	21	29	17
B lineage lymphoma	0	0	3 (89)	3 (52)
Thymic lymphoma	0	5 (121)	7 (122)	12 (79)
Teratoma	0	0	3 (50)	0
Sarcoma	0	1 (77)	4 (106)	3 (61)
Adenocarcinoma	0	0	0	1 (81)
Cause of death unknown	0	3 (129)	2 (19)	3 (61)

Shown is the number of cohort mice that succumbed to each tumor type. The numbers shown in parentheses indicate the average day at which mice were moribund and analyzed.

in p53-deficient mice (Supplemental Table S2), analyses of larger numbers of $H^{+/\Delta}P^{-/-}$ and $H^{+/+}P^{-/-}$ teratomas will be needed to evaluate relative contributions of H2AX haploinsufficiency versus p53 deficiency. Overall, we conclude that the $H2AX^{+/\Delta}$ genotype substantially accelerates tumorigenesis in a p53-deficient background, a conclusion further substantiated by detailed analyses of $H^{+/\Delta}P^{-/-}$ lymphomas (see below) and confirmed by an independent study (Celeste et al., 2003 [this issue of *Cell*]).

$H^{\Delta/\Delta}P^{-/-}$ and $H^{+/\Delta}P^{-/-}$ Thymic Lymphomas Contain Complex Translocations

SKY of early passage cells from seven $H^{\Delta/\Delta}P^{-/-}$ and two $H^{+/\Delta}P^{-/-}$ thymic lymphomas revealed striking chromosomal abnormalities in six $H^{\Delta/\Delta}P^{-/-}$ and one $H^{+/\Delta}P^{-/-}$ tumors, most notably translocations often involving several chromosomes (Figures 2A–2C; Supplemental Table S3). T cell lymphomas in $p53^{-/-}$ mice have been reported to generally lack chromosomal translocations (Liao et al., 1998), although extensive cytogenetics have not been reported. Thus, we conducted SKY on early passage cells from two $H^{+/+}P^{-/-}$ T cell lymphomas. In contrast to $H^{\Delta/\Delta}P^{-/-}$ tumors, both $H^{+/+}P^{-/-}$ T cell lymphomas lacked clonal translocations, although they did exhibit aneuploidy or a few nonclonal translocations (Supplemental Table S3; Supplemental Figure S4). Furthermore, SKY showed that two additional $p53^{-/-}$ thymic lymphomas from a parallel cohort also lacked clonal translocations (S. Rooney and F.W.A., unpublished data). We conclude that $H^{\Delta/\Delta}P^{-/-}$ and a subset of $H^{+/\Delta}P^{-/-}$ thymic lymphomas are distinct from those of older p53-deficient mice, not only in time of onset, but also in the frequent occurrence of dramatic genomic instability featuring complex chromosomal translocations.

Despite localization of RAG-dependent γ-H2AX foci to the TCRα locus during V(D)J recombination, we found only one translocation, which was nonclonal, involving chr 14 in the seven analyzed $H^{\Delta/\Delta}P^{-/-}$ thymic lymphomas (Supplemental Table S3). In addition, none of the $H^{\Delta/\Delta}P^{-/-}$ tumors harbored clonal translocations involving chr 6 or 13, which contain, respectively, the TCRβ and TCRγ loci. However, nearly all $H^{\Delta/\Delta}P^{-/-}$ tumors are $CD4^+/CD8^+$ or $CD4^-/CD8^+$ and also contain TCRβ gene rearrangements (Supplemental Table S3; data not shown). Therefore, it is likely that the complex translocations arise in association with TCRβ-triggered rapid cellular proliferation during DN to DP thymocyte expansion, rather than via aberrant V(D)J recombination.

$H^{\Delta/\Delta}P^{-/-}$ B Cell Lymphomas Contain IgH Locus Translocations and Complicons with Amplified c-*myc*

Based on SKY and fluoresence in situ hybridization (FISH), $H^{\Delta/\Delta}P^{-/-}$ pro-B cell lymphomas 590 and 698, like the vast majority of NHEJ-/p53-deficient pro-B cell lymphomas, had clonal, nonreciprocal C12;15 translocations, normal chr 12s, and, respectively, clonal C15;12;15 and C15;12;16 complicons (Figure 3C; Supplemental Table S5). Southern blotting with J_H probes revealed three nongermline J_H alleles, of which one was amplified, in both 590 and 698 cells (Figure 4A). Additional assays with an IgH 3′ regulatory region (IgH3′RR) probe and a c-*myc* probe revealed significant amplification of the entire 200 kb C_H region and confirmed c-*myc* amplification in both tumors (Figures 4B and 4C). Analyses of cloned, amplified 12;15 breakpoints from tumors 590 and 698 revealed fusion of J_H locus sequences, consistent with involvement of RAG-initiated DSBs, to regions 320 (590) and 160 (698) kb downstream of c-*myc* (Figures 5A and 5B). These translocations occurred in an orientation that would generate a dicentric 12;15 chromosome and that would promote c-*myc* amplification via a BFB mechanism (Zhu et al., 2002). The above features of $H^{\Delta/\Delta}P^{-/-}$ pro-B lymphoma complicons are shared with those of NHEJ-/p53-deficient pro-B cell lymphomas and imply a similar overall mechanism of origin (see Discussion). One difference, however, was that complicon junctions from $H^{\Delta/\Delta}P^{-/-}$ pro-B cell lymphomas lacked short sequence homologies and contained nucleotide additions (Figure 5B), indicating that they were catalyzed by classical NHEJ as opposed to a microhomology-based end-joining pathway.

SKY and FISH revealed that $H^{\Delta/\Delta}P^{-/-}$ B lineage lymphoma 888 had a C12;15;3 complicon containing amplified IgH and c-*myc* sequences, as well as a normal chr 12, but that it lacked the clonal C12;15 observed in the 590 and 698 $H^{\Delta/\Delta}P^{-/-}$pro-B cell tumors and in RAG-sufficient, NHEJ-/p53-deficient pro-B cell tumors (Figures 3A and 3B; Supplemental Table S5; Difilippantonio et al., 2002; Zhu et al., 2002). Southern blotting revealed two nonamplified J_H alleles and confirmed amplification of the 3′IgH RR and of c-*myc*, in agreement with FISH results (Figures 4A–4C). Furthermore, assays with an internal switch μ ($S\mu$) probe revealed several nongermline bands, including one with dramatic amplification (Figure 4D). This finding suggests that the amplified 12;15 breakpoint involved $S\mu$ rather than J_H sequences, an interpretation confirmed by preliminary nucleotide sequence analyses (data not shown). Consistent with a more advanced developmental stage, this tumor had a clonal Jκ rearrangement (Figure 4E). In this context, the $S\mu$-involved translocation event may have occurred on the productive IgH allele separating the V_HDJ_H rearrangement from Cμ and resulting in the loss of cell-surface IgM expression.

$H^{+/\Delta}P^{-/-}$ B Lymphomas Represent More Advanced Stages of B Cell Development

All three of the cohort $H^{+/\Delta}P^{-/-}$ B lineage tumors had characteristics of cells beyond the pro-B cell stage. $H^{+/\Delta}P^{-/-}$ tumor 855 was an $Ig\mu^+/IgL^-$ pre-B cell lymphoma with a complex, clonal C15;12;16 translocation that contained amplified IgH and c-*myc* sequences but which lacked a clonal C12;15 translocation (Figures 3D, 4B, and 4C; Supplemental Table S5). Southern blotting revealed two nonamplified, rearranged J_H alleles and two rearranged $S\mu$ regions, one of which was amplified (Figures 4A and 4D). Nucleotide sequencing of the amplified 855 junction revealed that $S\mu$ was rearranged precisely into an unmapped sequence (GA_x6K02T01LGS) on the Celera database (Figure 5B). Overall, these data indicate the 855 $H^{+/\Delta}P^{-/-}$ pre-B cell lymphoma contains an amplified 12;15 breakpoint involving $S\mu$ sequences and that, as in $H^{\Delta/\Delta}P^{-/-}$ B cell lymphoma 888, the amplified 12;15 translocation involving $S\mu$ was not associated with a clonal C12;15. $H^{+/\Delta}P^{-/-}$ tumor 464 was an IgM^-

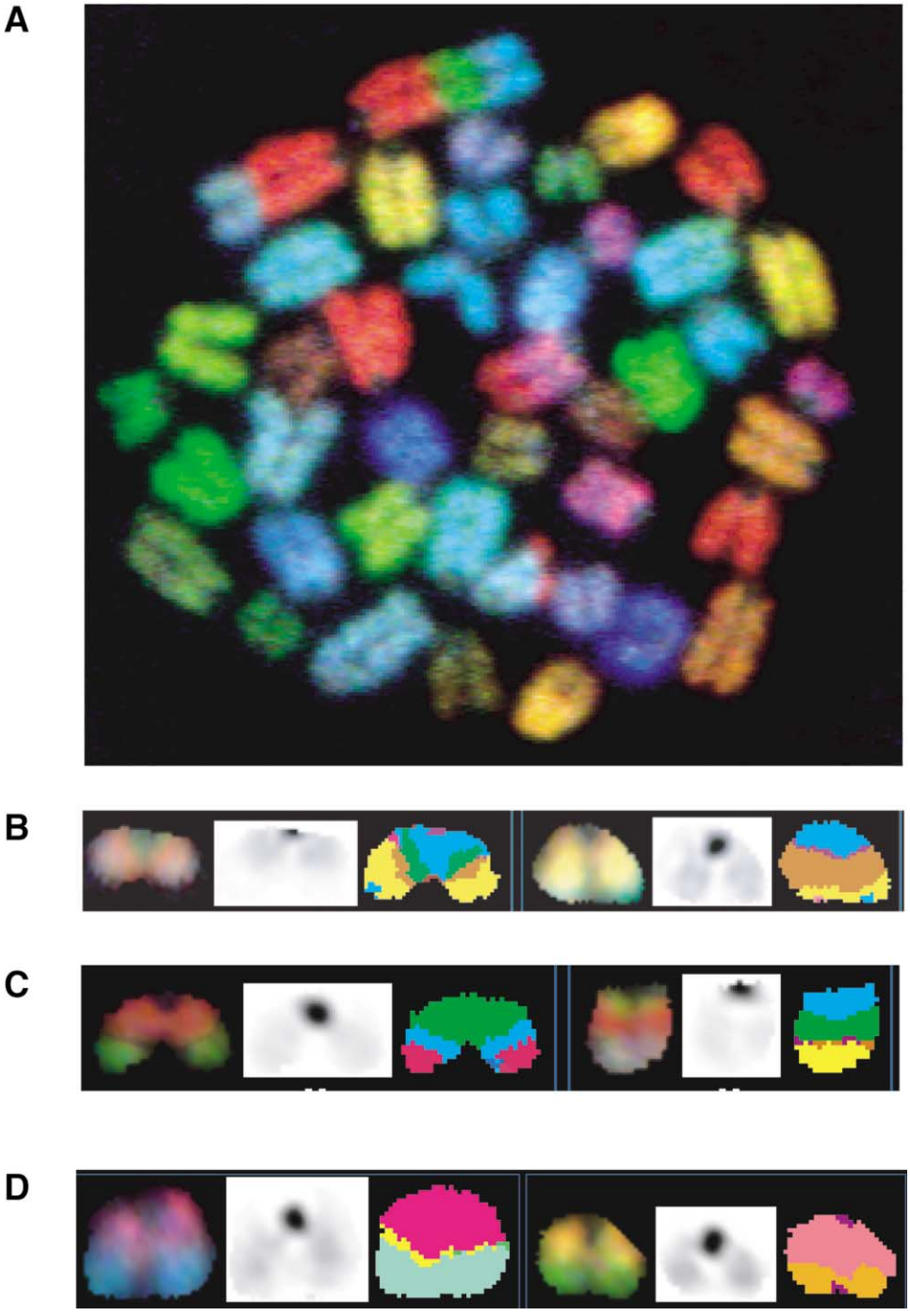

Figure 2. $H^{\Delta/\Delta}P^{-/-}$, $H^{+/\Delta}P^{-/-}$, and $H^{\Delta/\Delta}$ Thymic Lymphomas Harbor Clonal, Complex Translocations

(A–D) SKY images of a metaphase from $H^{+/\Delta}P^{-/-}$ thymic lymphoma 609 with C9;16;13, C12;9, C2;1, and C1;2 translocations (A) and images of representative translocations C11;10;1 (left) and C11;5;1 (right) from $H^{\Delta/\Delta}P^{-/-}$ thymic lymphoma 634 (B), C10;11;18 (left) and C11;10;1 (right) from $H^{\Delta/\Delta}P^{-/-}$ thymic lymphoma 603 (C), and the C12;15 (left) and C14;15 (right) translocations of $H^{\Delta/\Delta}$ thymic lymphoma 455 (D). SKY images are on the left, DAPI images in the middle, and computer-classified colors on the right (B–D).

B lineage tumor with a clonal, nonreciprocal C12;15 translocation and a clonal C12;2 translocation, neither of which harbored obviously amplified IgH or c-*myc* sequences (Figures 3E, 4B, and 4C; Supplemental Table S5). This tumor lacked a normal chr 12. Southern blotting revealed tumor 464 had two rearranged, nonamplified J_H sequences (Figure 4A) and deletions of IgH sequences on both chromosomes that extended from Sμ to, respectively, a region between Cδ and Sγ3 and a region between Sγ1 and the 3′ IgHRR (Figure 5A; data not shown). In addition, this tumor had two clonal Jκ rearrangements (Figure 4E). FISH with 3′IgH RR or

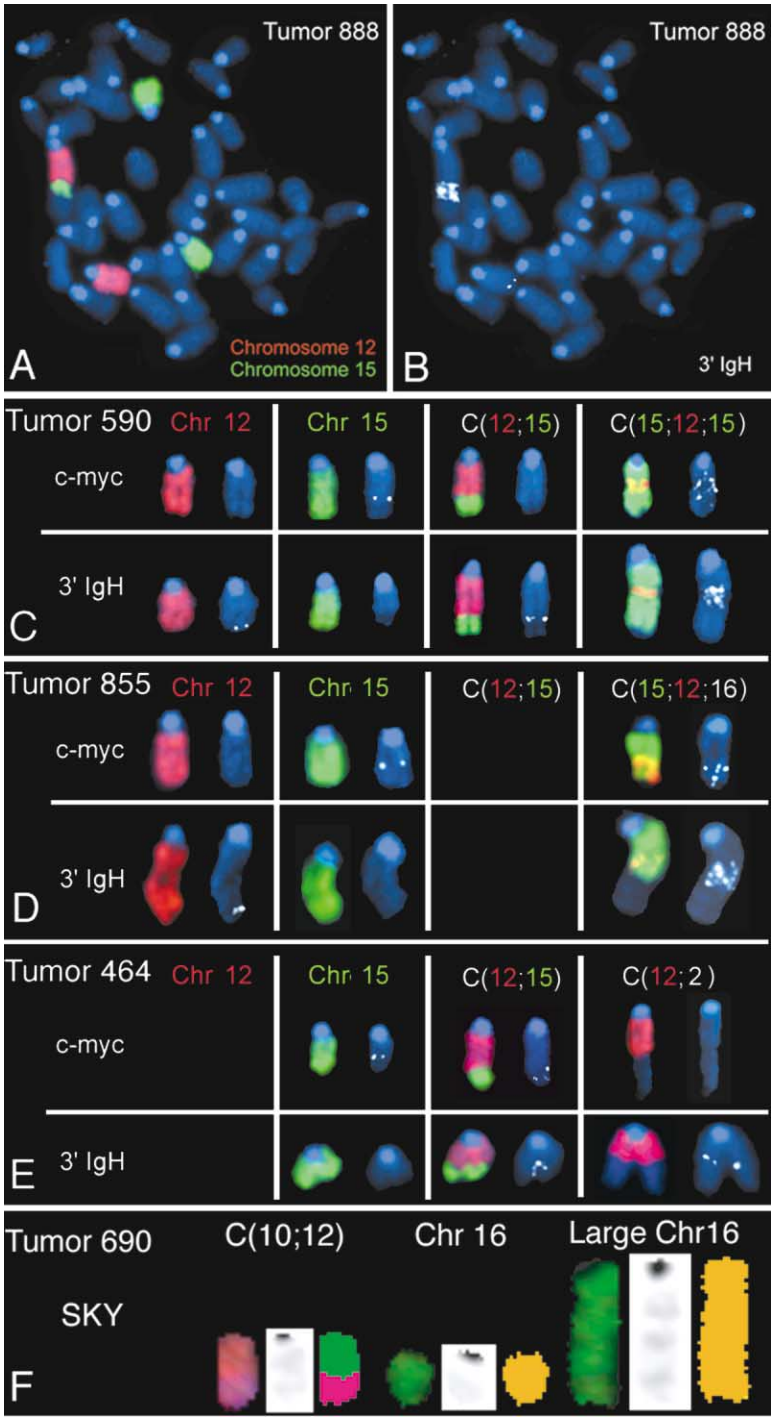

Figure 3. $H^{\Delta/\Delta}P^{-/-}$ and $H^{+/\Delta}P^{-/-}$ B Lymphomas Harbor Chr 12;15 Translocations with Coamplified IgH and c-*myc* or IgH Fused with c-*myc* Exon 1

(A–E) FISH analysis with chromosome paints and locus specific probes of $H^{\Delta/\Delta}P^{-/-}$ B cell lymphomas 888 (A and B) and 590 (C) and $H^{+/\Delta}P^{-/-}$ B cell lymphomas 855 (D) and 464 (E).

(F) SKY analysis showing the clonal C10;12 translocation, normal chr 16, and abnormally large chr 16 of $H^{+/\Delta}P^{-/-}$ mature B cell lymphoma 690. The SKY image is on the left, DAPI image in the middle, and computer classified colors on the right.

c-*myc* probes demonstrated that that downstream IgH locus sequences were located at the C12;15 and C12;2 translocation junctions and that c-*myc* exons 2 and 3 were located at the C12;15 junction, with potential duplication of both IgH and c-*myc* sequences (Figure 3E; data not shown). We cloned and sequenced the C12;15 translocation junction and confirmed that it involved IgH sequences between Cδ and Sγ3 fused into c-*myc* exon 1 in an orientation that would form a standard C12;15 translocation reminiscent of those found in Burkitt's lymphomas (Figures 5A and 5B).

The third B lineage tumor (690) that developed in $H^{+/\Delta}P^{-/-}$ mice was an $IgG1^{+}/IgL^{+}$ mature B cell lymphoma. SKY of 690 cells revealed a clonal C10;12 translocation and an aberrantly large chr 16 in every metaphase (Figure 3F; Supplemental Table S5). Southern blotting revealed two nongermline J_H alleles, neither of which was amplified (Figure 4A). In addition, Southern and FISH analyses revealed no amplification of the IgH region or c-*myc* (Figures 4B and 4C; data not shown).

We conclude that all currently characterized $H^{+/\Delta}P^{-/-}$ B lineage tumors are distinct from those observed in the context of NHEJ/p53 deficiency. They represent more mature stages of B cell development and also involve

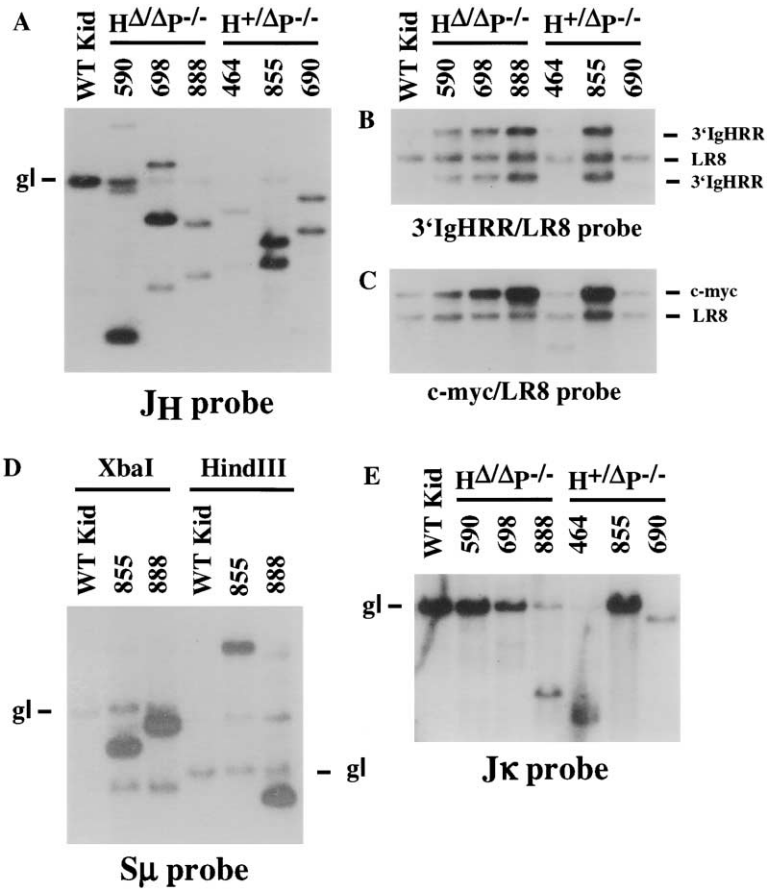

Figure 4. $H^{\Delta/\Delta}P^{-/-}$ and $H^{+/\Delta}P^{-/-}$ B Lymphomas Harbor Translocations Involving IgH and c-*myc* Sequences

(A–E) Southern blot analysis of tumor and normal kidney DNA with a J_H probe (A), a 3′IgHRR probe (B), a c-*myc* probe (C), a $S\mu$ probe (D), and a $J\kappa$ probe (E). The LR8 control probe was used as a control for loading (B and C) to indicate the amplification of C_H and c-*myc* sequences. All DNAs were digested with EcoRI unless otherwise indicated. The third c-*myc* hybridizing band in tumor 464 (C) represents a subclonal C15;9 translocation.

translocations into chr 12 regions well downstream of the J_H region.

H2AX Haploinsufficiency Predisposes to Cancer in a p53-Deficient Background

Classical tumor suppressor genes lead to cancer following loss of heterozygosity (LOH) and inactivation of both allelic copies (Knudson, 1971). However, inactivation of just one copy of certain genes (haploinsufficiency) also may predispose to cancer (Fodde and Smits, 2002). To distinguish these possibilities with respect to $H^{+/\Delta}P^{-/-}$ tumors, we first examined the H2AX locus in $H^{+/\Delta}P^{-/-}$ B cell lymphomas 464, 855, and 690. Southern blotting with a probe that hybridizes 3′ of the H2AX gene and distinguishes the $H2AX^{+}$ and $H2AX^{\Delta}$ alleles revealed all three $H^{+/\Delta}P^{-/-}$ lymphomas maintained the wild-type H2AX allele (data not shown). Furthermore, we used PCR to isolate and sequence the H2AX gene from $H^{+/\Delta}P^{-/-}$ B cell lymphomas 464 and 855 and found no mutations within the coding region (data not shown). Finally, Western analyses revealed that H2AX was expressed in all three $H^{+/\Delta}P^{-/-}$ B cell lymphomas, as well as in several $H^{+/\Delta}P^{-/-}$ T cell lymphomas (Figure 6A). We conclude that H2AX haploinsufficiency in a p53-deficient background leads both to an increased tumor incidence and the appearance of novel cancers.

H2AX Haploinsufficiency Leads to Increased Genomic Instability in Normal Lymphocytes

To investigate the cellular consequences of H2AX haploinsufficiency, we analyzed expression of H2AX in $H2AX^{+/+}$, $H2AX^{+/\Delta}$, and $H2AX^{\Delta/\Delta}$ thymocytes and found that $H2AX^{+/\Delta}$ thymocytes express approximately half the level of H2AX protein as $H2AX^{+/+}$ thymocytes (Figure 6B). To evaluate whether H2AX haploinsufficiency results in genomic instability in normal lymphocytes, we examined the cytogenetic consequences of monoallelic H2AX expression by DAPI analyses of stimulated $H2AX^{+/+}$, $H2AX^{+/\Delta}$, and $H2AX^{\Delta/\Delta}$ splenic T cells. Approximately half (52% ± 7%) of the $H2AX^{\Delta/\Delta}$ T cells exhibited chromosomal abnormalities (Figure 6C), including chromosomal gaps, fusions, fragments, and detached centromeres, while only about 10% (11% ± 3%) of $H2AX^{+/+}$ cells contained chromosome abnormalities (Figure 6C) ($H2AX^{+/+}$ versus $H2AX^{\Delta/\Delta}$, $p = 0.001$). However, approximately one-third (30% ± 4%) of the $H2AX^{+/\Delta}$ T cells exhibited chromosomal aberrations (Figure 6C) ($H2AX^{+/+}$ versus $H2AX^{+/\Delta}$, $p = 0.008$), demonstrating that biallelic expression of H2AX is required for full maintenance of genomic stability in normal proliferating T lymphocytes. Similar conclusions were reached from analyses of cells from an independently generated H2AX-deficient mouse (Celeste et al., 2003).

Discussion

The Function of H2AX in DSB Repair and Tumor Suppression

Deficiency for histone H2AX, a core chromatin component, leads to a markedly increased predisposition to various tumors in the context of p53 deficiency. Moreover, $H^{\Delta/\Delta}P^{-/-}$ and $H^{+/\Delta}P^{-/-}$ lymphoid tumors routinely

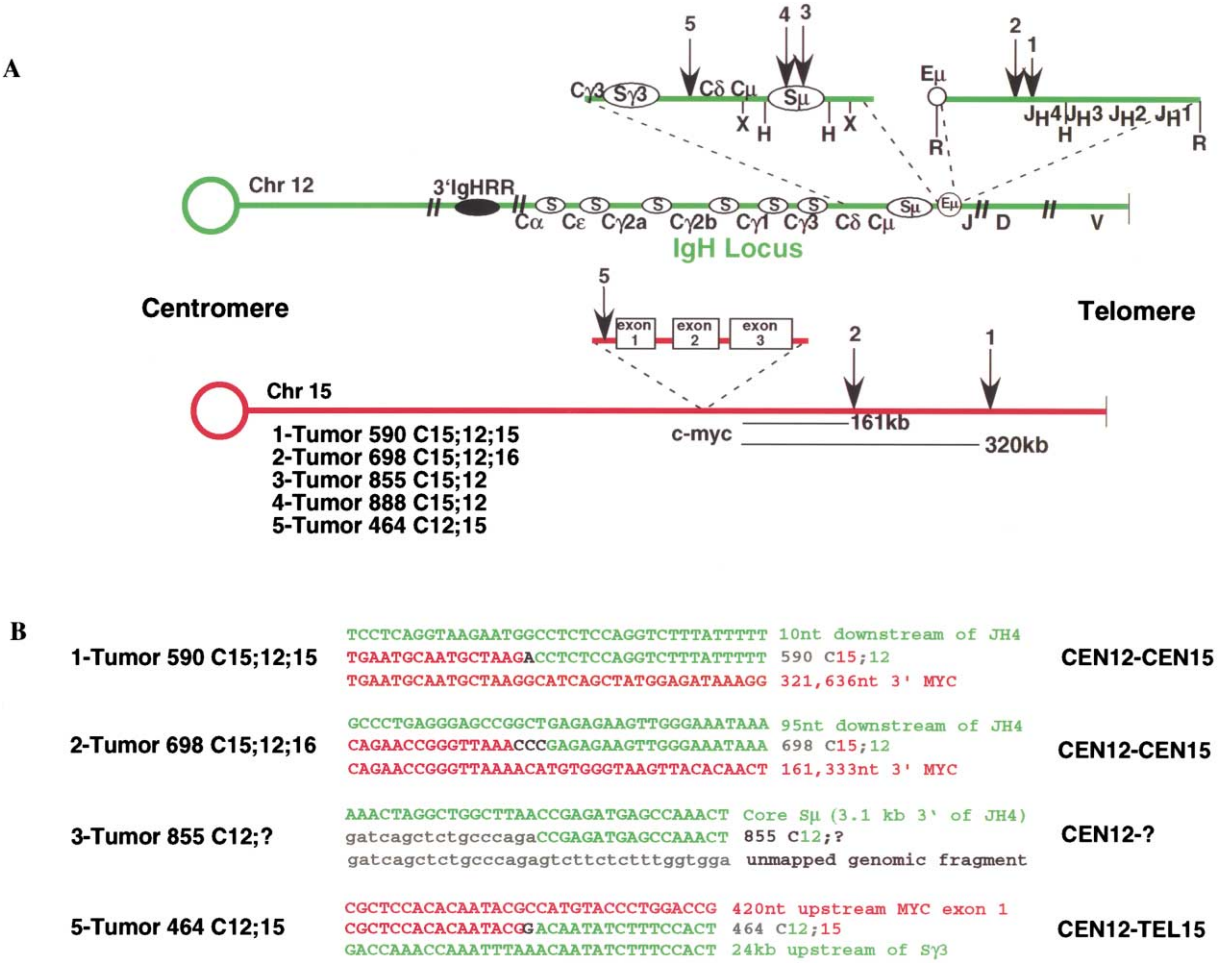

Figure 5. IgH Locus Translocation Breakpoints of $H^{\Delta/\Delta}P^{-/-}$ and $H^{+/\Delta}P^{-/-}$ B Lineage Lymphomas

(A) Schematic representation of where the 12;15 breakpoints (1–5) of indicated tumors map (arrows) within the IgH locus (chr 12) and c-*myc* (chr 15).

(B) Sequences of the cloned breakpoints of the 590 and 698 complicons, an amplified junction from tumor 855, and the C12;15 translocation of tumor 464. Chr 12 sequences are in green, chr 15 sequences in red, and N nucleotides in black. Unmapped genomic sequences are indicated in lowercase black letters.

exhibit dramatic genomic instability highlighted by clonal translocations that, depending on tumor type, are likely due to G1 defects, S/G2 defects, or both. These findings are consistent with the notion that phosphorylated H2AX flanking DSBs has a role in multiple cell cycle phases that could include recruitment or organization of repair factors (Celeste et al., 2002; Fernandez-Capetillo et al., 2002; Paull et al., 2000; Rogakou et al., 1999). The finding that H2AX haploinsufficiency also results in increased genomic instability and cancer incidence, in the absence of p53, is particularly intriguing and has both clinical (see below) and mechanistic implications. Thus, normal (biallelic) H2AX expression levels are crucial for its functions. While there are several possibilities, the H2AX dosage effect may reflect its structural role in chromatin. H2AX represents about 15% of cellular H2A, and there are two H2A molecules per nucleosome. Thus, H2AX should be present, on average, in about one of three nucleosomes, and this density might be expected to drop in haploinsufficient cells. In the context of chromatin, such a density drop may not allow H2AX to effectively perform its requisite functions.

$H^{\Delta/\Delta}P^{-/-}$ mice die largely of very rapid onset thymic lymphomas, although pro-B lymphomas and solid tumors also were observed. $H^{+/\Delta}P^{-/-}$ mice have a later onset of thymic lymphomas that, on average, still was earlier than that of $p53^{-/-}$ mice (Supplemental Table S2). As one of two $H^{+/\Delta}P^{-/-}$ lymphomas analyzed harbored complex translocations and the other was just aneuploid (Supplemental Table S2), some $H^{+/\Delta}P^{-/-}$ thymic lymphomas may arise due to combined effects of reduced H2AX plus p53 deficiency, while others arise simply from lack of p53. $H^{+/\Delta}P^{-/-}$ mice, in part due to reduced incidence of thymic lymphomas, show a relatively broad spectrum of tumors, including more mature B lineage lymphomas and frequent sarcomas. Presumably, $H^{\Delta/\Delta}P^{-/-}$ mice also would show a greater predisposition to such tumors if spared from early T and pro-B cell lymphomas via conditional H2AX inactivation. There was, however, one distinct difference in the tumor spectrum of $H^{+/\Delta}P^{-/-}$

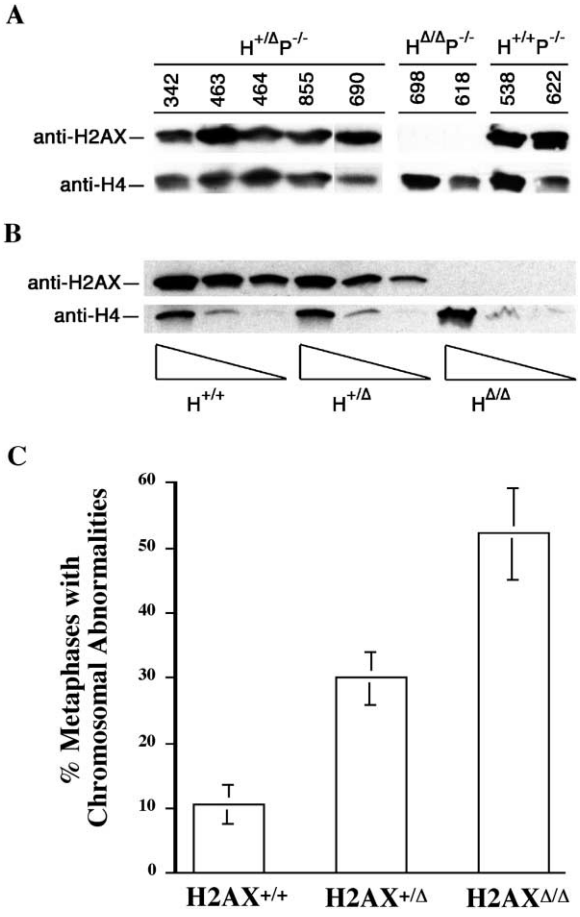

Figure 6. H2AX Haploinsufficiency Predisposes Cells to Tumorigenesis

(A and B) Western analysis of (A) H2AX expression (anti-H2AX) in $H^{+/+}P^{-/-}$, $H^{+/\Delta}P^{-/-}$, and $H^{\Delta/\Delta}P^{-/-}$ lymphomas and (B) serial 2-fold dilutions of total protein of $H^{+/+}$, $H^{+/\Delta}$, and $H^{\Delta/\Delta}$ thymocytes. Histone H4 (anti-H4) levels control for sample loading.

(C) Graph representing the average percent of $H^{+/+}$, $H^{+/\Delta}$, and $H^{\Delta/\Delta}$ T cell metaphases with chromosomal abnormalities obtained from four independent experiments.

mice relative to $H^{\Delta/\Delta}P^{-/-}$ mice; frequent, early-onset germ cell tumors in male $H^{+/\Delta}P^{-/-}$ mice were not observed in male $H^{\Delta/\Delta}P^{-/-}$ mice. In this regard, complete H2AX-deficiency blocks meiosis and p53-deficiency does not rescue this process (Fernandez-Capetillo et al., 2003); thus, ablation of germ cell development in male $H^{\Delta/\Delta}P^{-/-}$ mice may suppress any potential to generate germ cell tumors that might result from combined absence of H2AX and p53.

In mammalian cells, H2AX has been implicated in S and G2 repair via HR (Bassing et al., 2002a; Celeste et al., 2002). However, a potential role in G1 and NHEJ was suggested by localization of H2AX foci to the TCRα locus during V(D)J recombination (Chen et al., 2000). We now show that H2AX, indeed, is required for fully normal ability to process G1 phase DSBs in the context of V(D)J recombination, based on our finding of $H^{\Delta/\Delta}P^{-/-}$ pro-B cell lymphomas with both signature C12;15 translocations and related complicons derived from J_H translocations. Such sets of chromosomal anomalies likely result from replication and subsequent misrepair of G1 phase DSBs generated by RAG (Zhu et al., 2002) and were observed previously only in the context of NHEJ and p53 deficiency (Difilippantonio et al., 2002; Gladdy et al., 2003; Zhu et al., 2002). H2AX may suppress RAG-initiated chromosomal translocations by facilitating NHEJ access to or otherwise functioning in synapsis of RAG-liberated ends. H2AX could also suppress RAG-initiated translocations by participating in G1 checkpoints to ensure repair of all DSBs before S phase entry. In this regard, H2AX was reported to have a G2/M checkpoint role in the context of low level DNA damage (Fernandez-Capetillo et al., 2002). In addition, S phase H2AX functions might contribute to suppression of G1-initiated translocations by eliminating potential recombination targets for persisting RAG-generated ends. Such functions might include a putative role downstream of ATM or ATR, possibly in resolution of stalled replications forks or in maintenance of fragile-site stability (Casper et al., 2002; Ward and Chen, 2001).

H2AX-Deficient and Haploinsufficient Lymphoid Tumors

$H^{\Delta/\Delta}P^{-/-}$ thymic lymphomas arise very early and do not, despite numerous clonal translocations, routinely have translocations involving chromosomes that harbor TCR loci. Therefore, $H^{\Delta/\Delta}P^{-/-}$ thymic lymphomas may involve chromosomal abnormalities that arise via aberrant repair of general DSBs in rapidly dividing, developing thymocytes; this might mask lymphomas that could arise later in development due to TCRα translocations. H2AX/p53 deficiency may lead to S phase abnormalities via defective BRCA1-mediated repair in the absence of H2AX and lack of Chk2-mediated apoptosis in the absence of p53 (Bachelier et al., 2003; Hirao et al., 2002; Jack et al., 2002; Mak et al., 2000). Another possibility would involve reduced ability to form 53BP1/MDC1 foci required for complete activation of S phase checkpoints following DSBs (Goldberg et al., 2003; Lou et al., 2003; Stewart et al., 2003; Wang et al., 2002; Ward et al., 2003). Most $H^{\Delta/\Delta}P^{-/-}$ thymic lymphomas have a TCR$\alpha\beta$-negative, DP phenotype. Thus, as normal DP thymocytes require $\alpha\beta$ TCR-mediated selection for survival (Anderson et al., 1999), $H^{\Delta/\Delta}P^{-/-}$ thymic lymphomas may arise from DP cells or earlier stage lymphoma stem cells via genetic or epigenetic changes that sustain self-renewal or lack of apoptosis. It is curious that $H^{\Delta/\Delta}P^{-/-}$ thymic lymphomas do not arise secondarily to TCRβ locus translocations, despite the contribution of J_H rearrangements to $H^{\Delta/\Delta}P^{-/-}$ pro-B cell lymphomas. In fact, translocations involving TCRβ are infrequent in murine lymphomas. In this regard, the TCRβ locus may lack capacity to effectively activate linked oncogenes, as opposed to the IgH or TCRα loci that have long-range enhancers (Cogne et al., 1994; Sleckman et al., 1997). In addition, given the larger target cell pool, translocations occurring during rapid expansion after a productive TCRβ rearrangement may swamp out potential translocations involving TCRβ locus rearrangement. Such scenarios also would explain the absence of T cell lymphomas in NHEJ-/p53-deficient mice, as the NHEJ defect does not allow DN T cells to generate TCRβ chains to drive expansion or progression to TCRα locus rearrangement.

$H^{\Delta/\Delta}P^{-/-}$ pro-B cell lymphomas had translocated J_H region sequences with deletions reminiscent of those found in NHEJ-/p53-deficient pro-B cell lymphomas, despite the majority of DJ_H joins being normal in $H^{\Delta/\Delta}P^{-/-}$ lymphocytes. Thus, H2AX-deficiency may allow occasional J_H ends to escape joining in G1 and (in the absence of p53) undergo replication, which could result in deletions of J_H ends (Zhu et al., 2002). Then, such replicated DSBs may be translocated to S phase-generated lesions associated with H2AX deficiency, for example, from putative fragile sites downstream of c-*myc*, to generate C12;15 (marker) and dicentric (complicon) 12;15 chromosomal junctions. NHEJ-/p53-deficient lymphomas are clonal, consistent with additional mutation(s) being required for transformation. In this context, *H2AX* maps to a region of chr 9 that, by comparative genomic hybridization, appears frequently deleted in NHEJ-/p53-deficient pro-B cell lymphomas (Zhu et al., 2002; Celera database). Conceivably, reduced H2AX levels also might contribute to translocation of RAG-initiated DSBs in NHEJ-/p53 pro-B cells by facilitating generation of S phase acceptor ends for replicated RAG-initiated DSBs. Finally, a microhomology-based end-joining pathway catalyzed complicon junctions in NHEJ-/p53-deficient pro-B cell lymphomas (Zhu et al., 2002). In contrast, translocation junctions in $H^{\Delta/\Delta}P^{-/-}$ pro-B cell lymphomas appeared to be catalyzed by classical NHEJ. Recent studies have shown that telomere fusions also can be catalyzed by NHEJ (Smogorzewska et al., 2002). Thus, chromosome translocations can be catalyzed by HR (Bosco and Haber, 1998), microhomology-based end-joining (Zhu et al., 2002), and classical NHEJ.

No breakpoints associated with defective CSR were found in a large number of NHEJ-/p53-deficient pro-B cell lymphomas (Difilippantonio et al., 200; Zhu et al., 2002). However, unlike NHEJ-/p53-deficient mice, H2AX-/p53-deficient mice generate more mature B-lineage cells that might have potential to acquire genomic instability due to impaired IgH CSR. Our analyses of $H^{\Delta/\Delta}P^{-/-}$ and $H^{+/\Delta}P^{-/-}$ B lineage lymphomas support this notion. Thus, $H^{\Delta/\Delta}P^{-/-}$ lymphoma 888 and $H^{+/\Delta}P^{-/-}$ lymphoma 464 have Igκ rearrangements and 12;15 chromosomal translocations in which apparent chr 12 breakpoints are well downstream of J_H, with one (888), which harbored a 12;15 complicon, having an amplified Sμ junction and the other (464), which had a C12;15 translocation, having a junction downstream of Sμ and Cδ into c-*myc* exon 1. In addition, $H^{+/\Delta}P^{-/-}$ pre-B cell lymphoma 855, which had a 12;15 complicon, also harbored an amplified Sμ junction. Notably, both $H^{\Delta/\Delta}P^{-/-}$ tumor 888 and $H^{+/\Delta}P^{-/-}$ tumor 855, despite having a 12;15 complicon, lacked the companion C12;15 "signature" translocation of replicated DSBs, potentially suggesting that the putative initiating lesions in Sμ might have occurred in S phase. Overall, these findings suggest that conditional inactivation of H2AX in mature B cells may provide the basis for a model of mature B cell lymphomas that arise in association with aberrant CSR.

Potential Relevance of H2AX Deficiency or Haploinsufficiency to Human Cancer

Human *H2AX* (*H2AFX*) maps 11 Mb telomeric of *ATM* on chromosome 11 at 11q23, a region that exhibits LOH or deletion in a large number of human cancers (Supplemental Table S1). Moreover, *H2AFX* maps within the minimal regions of LOH or deletion that have been defined in a number of studies involving a wide variety of human cancers (Supplemental Table 1). Such findings have led to the proposal that the 11q23 region contains a human tumor suppressor gene(s) in addition to *ATM*. Thus, our finding that H2AX functions as a tumor suppressor in mice clearly identifies *H2AFX* as a strong candidate for such an additional tumor suppressor gene within the 11q23 region. Analysis of *H2AFX* sequence in a panel of breast cancers revealed an intact *H2AFX* gene (Monteiro et al., 2003). However, our mouse studies show that haploinsufficient H2AX expression dramatically predisposes to genomic instability and, in the context of p53 deficiency, cancer. As many human lymphomas and solid tumors contain deletions of 11q23 on a single allele (Supplemental Table S1), loss of a single copy of *H2AFX* might play a role in unleashing genetic instability in humans. For example, *H2AFX* lies approximately 0.6 Mb telomeric of the *MLL* gene; thus, the 0.6–0.7 Mb deletions that often extend 3′ of *MLL* in human leukemias with 11q23 translocations involving *MLL* (Cherif et al., 1994) theoretically could contribute to tumorigenesis through loss of a single copy of *H2AFX*. Moreover, deletions that generate LOH of *ATM* (which regulates p53) in tumors such as mantle cell lymphoma and B cell chronic lymphocytic lymphoma (Schaffner et al., 1999; Stilgenbauer et al., 1999), may have more severe genomic consequences if a single copy of *H2AFX* is also inactivated. Clearly, it will be important to examine the status of both copies of *H2AFX* in human cancers exhibiting 11q23 alterations, especially those with marked genetic instability or recurrent translocations.

Experimental Procedures

Generation of Mice

$H2AX^{+/\Delta}$ ES cells (Bassing et al., 2002a) were used to generate 129Sv $H2AX^{\Delta/\Delta}$ and $H2AX^{+/\Delta}$ mice. 129Sv $H2AX^{+/\Delta}$ and 129Sv/C57BL/6 $p53^{-/-}$ mice (Donehower et al., 1992) were bred to generate $H^{+/\Delta}P^{+/-}$ mice, which were interbred to generate cohort mice.

Characterization of Tumors

Lymphomas were characterized by flow cytometry using anti-CD4, CD8, CD3, B220, IgM, CD43, Igλ, Igκ, IgG1 (Pharmingen), and anti-IgM (Southern Biotech) antibodies. Solid tumors were characterized via H & E staining. B cell lymphoma cultures were grown as described (Zhu et al., 2002) or with LPS (Pharmingen) instead of IL7. Metaphase preparation, chromosome painting, SKY, and FISH analyses were conducted as described (Zhu et al., 2002). The 3′IgH RR FISH probe was a BAC (199M11) comprised of sequence that extends from Cα through the 3′IgH RR (Research Genetics). The J_H probe is a HindIII/EcoRI genomic fragment containing J_H4. The Sμ probe is a HindIII Sμ genomic fragment. The 3′IgHRR Southern probe is a 700 bp BamHI fragment just 3′ of Cα.

Cloning and Sequencing of Translocation Junctions

Complicon junctions, DJ_H, and V_HDJ_H rearrangements were cloned by PCR and sequenced as described (Zhu et al., 2002). The 464 and 590 C12;15 junctions were cloned using, respectively, the lambda DASH II vector and the lambda ZAP II vector (Stratagene).

Western Analyses

Tumor cells and normal thymocytes were lysed in Laemmli buffer and blotting conducted as described (Bassing et al., 2002a).

Genomic Instability Assays

Splenocytes were stimulated with ConA and IL2 for 48 hr (Sleckman et al., 1997) and metaphases prepared and analyzed as described (Bassing et al., 2002a). Assays were performed five times with $H^{+/+}$, $H^{+/\Delta}$, and $H^{\Delta/\Delta}$ thymocytes in either wild-type (three times) or $p53^{-/-}$ (two times) backgrounds. One experiment ($p53^{-/-}$) was disregarded as 32% of metaphases from putative wild-type cells contained abnormalities, including those only seen in $H^{+/\Delta}$ and $H^{\Delta/\Delta}$ thymocytes in the other four experiments, suggesting a potential sample error.

Acknowledgments

We thank Andre Nussenzweig for discussions of unpublished data and Connie Gee for advice on tumor database analyses. We thank Lianne Kaylor, Nicole Stokes, Caitlin Kennedy, and Yuko Fujiwara for technical assistance and Ali Zarrin for the 3′IgH RR BAC. We thank Li Zhang, Andrew Thompson, Gennifer Griffen, and Montserrat Michelman of the DFHCC Rodent Histopathology Core for dissections and slide preparation. D.O.F. is supported by NIH K08 HL67580-03. A Pfizer Postdoctoral Fellowship in Rheumatology/Immunology supports K.F.C. J.M. is supported by a Lymphoma Research Foundation fellowship. C.H.B. was an Irvington Institute for Immunological Research fellow and an Associate of the Howard Hughes Medical Institute. F.W.A. is an Investigator of the Howard Hughes Medical Institute. This work was supported by NIH grants AI35714 and NCI CA92625.

Received: May 2, 2003
Revised: June 18, 2003
Accepted: July 8, 2003
Published: August 7, 2003

References

Anderson, G., Hare, K.J., and Jenkinson, E.J. (1999). Positive selection of thymocytes: the long and winding road. Immunol. Today *20*, 463–468.

Bachelier, R., Xu, X., Wang, X., Li, W., Naramura, M., Gu, H., and Deng, C.X. (2003). Normal lymphocyte development and thymic lymphoma formation in *Brca1* exon-11-deficient mice. Oncogene *22*, 528–537.

Bassing, C.H., Chua, K.F., Sekiguchi, J., Suh, H., Whitlow, S.R., Fleming, J.C., Monroe, B.C., Ciccone, D.N., Yan, C., Vlasakova, K., et al. (2002a). Increased ionizing radiation sensitivity and genomic instability in the absence of histone H2AX. Proc. Natl. Acad. Sci. USA *99*, 8173–8178.

Bassing, C.H., Swat, W., and Alt, F.W. (2002b). The mechanism and regulation of chromosomal V(D)J recombination. Cell *109* (*Suppl*), S45–S55.

Bosco, G., and Haber, J.E. (1998). Chromosome break-induced DNA replication leads to nonreciprocal translocations and telomere capture. Genetics *150*, 1037–1047.

Brown, E.J., and Baltimore, D. (2003). Essential and dispensable roles of ATR in cell cycle arrest and genome maintenance. Genes Dev. *17*, 615–628.

Burma, S., Chen, B.P., Murphy, M., Kurimasa, A., and Chen, D.J. (2001). ATM phosphorylates histone H2AX in response to DNA double-strand breaks. J. Biol. Chem. *276*, 42462–42467.

Casper, A.M., Nghiem, P., Arlt, M.F., and Glover, T.W. (2002). ATR regulates fragile site stability. Cell *111*, 779–789.

Celeste, A., Petersen, S., Romanienko, P.J., Fernandez-Capetillo, O., Chen, H.T., Sedelnikova, O.A., Reina-San-Martin, B., Coppola, V., Meffre, E., Difilippantonio, M.J., et al. (2002). Genomic instability in mice lacking histone H2AX. Science *296*, 922–927.

Celeste, A., Difilippantonio, S., Difilippantonio, M.J., Fernandez-Capetillo, O., Pilch, D.R., Sedelnikova, O.A., Eckhaus, M., Ried, T., Bonner, W.M., and Nussenzweig, A. (2003). H2AX haploinsufficiency modifies genomic stability and tumor susceptibility. Cell *114*, this issue, 371–383.

Chen, H.T., Bhandoola, A., Difilippantonio, M.J., Zhu, J., Brown, M.J., Tai, X., Rogakou, E.P., Brotz, T.M., Bonner, W.M., Ried, T., and Nussenzweig, A. (2000). Response to RAG-mediated VDJ cleavage by NBS1 and γ-H2AX. Science *290*, 1962–1965.

Cherif, D., Bernard, O., Paulien, S., James, M.R., Le Paslier, D., and Berger, R. (1994). Hunting 11q23 deletions with fluorescence in situ hyridization (FISH). Leukemia *8*, 578–586.

Cogne, M., Lansford, R., Bottaro, A., Zhang, J., Gorman, J., Young, F., Cheng, H.L., and Alt, F.W. (1994). A class switch control region at the 3′ end of the immunoglobulin heavy chain locus. Cell *77*, 737–747.

Difilippantonio, M.J., Petersen, S., Chen, H.T., Johnson, R., Jasin, M., Kanaar, R., Ried, T., and Nussenzweig, A. (2002). Evidence for replicative repair of DNA double-strand breaks leading to oncogenic translocation and gene amplification. J. Exp. Med. *196*, 469–480.

Donehower, L.A., Harvey, M., Slagle, B.L., McArthur, M.J., Montgomery, C.A., Jr., Butel, J.S., and Bradley, A. (1992). Mice deficient for p53 are developmentally normal but susceptible to spontaneous tumours. Nature *356*, 215–221.

Downs, J.A., Lowndes, N.F., and Jackson, S.P. (2000). A role for *Sacchromyces cerevisiae* histone H2A in DNA repair. Nature *408*, 1001–1004.

Fernandez-Capetillo, O., Chen, H.T., Celeste, A., Ward, I., Romanienko, P.J., Morales, J.C., Naka, K., Xia, Z., Camerini-Otero, R.D., Motoyama, N., et al. (2002). DNA damage-induced G2-M checkpoint activation by histone H2AX and 53BP1. Nat. Cell Biol. *4*, 993–997.

Fernandez-Capetillo, O., Mahadevaiah, S.K., Celeste, A., Romanienko, P.J., Camerini-Otero, R.D., Bonner, W.M., Manova, K., Burgoyne, P., and Nussenzweig, A. (2003). H2AX Is required for chromatin remodeling and inactivation of sex chromosomes in male mouse meiosis. Dev. Cell *4*, 497–508.

Fodde, R., and Smits, R. (2002). A matter of dosage. Science *298*, 761–763.

Furuta, T., Takemura, H., Liao, Z.Y., Aune, G.J., Redon, C., Sedelnikova, O.A., Pilch, D.R., Rogakou, E.P., Celeste, A., Chen, H.T., et al. (2003). Phosphorylation of histone H2AX and activation of Mre11, Rad50, and Nbs1 in response to replication-dependent DNA-double-strand breaks induced by mammalian DNA topoisomerase I cleavage complexes. J. Biol. Chem. *278*, 20303–20312.

Gladdy, R.A., Taylor, M.D., Williams, C.J., Grandal, I., Karaskova, J., Squire, J.A., Rutka, J.T., Guidos, C.J., and Danska, J.S. (2003). The RAG-1/2 endonuclease causes genomic instability and controls CNS complications of lymphoblastic leukemia in p53/Prkdc-deficient mice. Cancer Cell *3*, 37–50.

Goldberg, M., Stucki, M., Falck, J., D'Amours, D., Rahman, D., Pappin, D., Bartek, J., and Jackson, S.P. (2003). MDC1 is required for the intra-S-phase DNA damage checkpoint. Nature *421*, 952–956.

Harvey, M., McArthur, M.J., Montgomery, C.A., Jr., Bradley, A., and Donehower, L.A. (1993). Genetic background alters the spectrum of tumors that develop in p53-deficient mice. FASEB J. *7*, 938–943.

Hirao, A., Cheung, A., Duncan, G., Girard, P.M., Elia, A.J., Wakeham, A., Okada, H., Sarkissian, T., Wong, J.A., Sakai, T., et al. (2002). Chk2 is a tumor suppressor that regulates apoptosis in both an ataxia telangiectasia mutated (ATM)-dependent and an ATM-independent manner. Mol. Cell. Biol. *22*, 6521–6532.

Jack, M.T., Woo, R.A., Hirao, A., Cheung, A., Mak, T.W., and Lee, P.W. (2002). Chk2 is dispensable for p53-mediated G1 arrest but is required for a latent p53-mediated apoptotic response. Proc. Natl. Acad. Sci. USA *99*, 9825–9829.

Jacks, T., Remington, L., Williams, B.O., Schmitt, E.M., Halachmi, S., Bronson, R.T., and Weinberg, R.A. (1994). Tumor spectrum analysis in p53-mutant mice. Curr. Biol. *4*, 1–7.

Jackson, S.P. (2002). Sensing and repairing DNA double-strand breaks. Carcinogenesis *23*, 687–696.

Knudson, A.G., Jr. (1971). Mutation and cancer: statistical study of retinoblastoma. Proc. Natl. Acad. Sci. USA *68*, 820–823.

Liao, M.J., Zhang, X.X., Hill, R., Gao, J., Qumsiyeh, M.B., Nichols, W., and Van Dyke, T. (1998). No requirement for V(D)J recombination in p53-deficient thymic lymphoma. Mol. Cell. Biol. *18*, 3495–3501.

Liyanage, M., Weaver, Z., Barlow, C., Coleman, A., Pankratz, D.G.,

Anderson, S., Wynshaw-Boris, A., and Ried, T. (2000). Abnormal rearrangement within the α/δ T-cell receptor locus in lymphomas from Atm-deficient mice. Blood *96*, 1940–1946.

Lou, Z., Minter-Dykhouse, K., Wu, X., and Chen, J. (2003). MDC1 is coupled to activated CHK2 in mammalian DNA damage response pathways. Nature *421*, 957–961.

Mahadevaiah, S.K., Turner, J.M., Baudat, F., Rogakou, E.P., de Boer, P., Blanco-Rodriguez, J., Jasin, M., Keeney, S., Bonner, W.M., and Burgoyne, P.S. (2001). Recombinational DNA double-strand breaks in mice precede synapsis. Nat. Genet. *27*, 271–276.

Mak, T.W., Hakem, A., McPherson, J.P., Shehabeldin, A., Zablocki, E., Migon, E., Duncan, G.S., Bouchard, D., Wakeham, A., Cheung, A., et al. (2000). Brca1 required for T cell lineage development but not TCR loci rearrangement. Nat. Immunol. *1*, 77–82.

Manis, J.P., Tian, M., and Alt, F.W. (2002). Mechanism and control of class-switch recombination. Trends Immunol. *23*, 31–39.

Mills, K.D., Ferguson, D.O., and Alt, F.W. (2003). The role of DNA breaks in genomic instability and tumorigenesis. Immunol. Rev. *194*, 77–95.

Monteiro, A.N., Zhang, S., Phelan, C.M., and Narod, S.A. (2003). Absence of constitutional H2AX gene mutations in 101 hereditary breast cancer families. J. Med. Genet. *40*, e51.

Nottenburg, C., St. John, T., and Weissman, I.L. (1987). Unusual immunoglobulin DNA sequences from the nonexpressed chromosome of mouse normal B lymphocytes: implications for allelic exclusion and the DNA rearrangement process. J. Immunol. *139*, 1718–1726.

Paull, T.T., Rogakou, E.P., Yamazaki, V., Kirchgessner, C.U., Gellert, M., and Bonner, W.M. (2000). A critical role for histone H2AX in recruitment of repair factors to nuclear foci after DNA damage. Curr. Biol. *10*, 886–895.

Petersen, S., Casellas, R., Reina-San-Martin, B., Chen, H.T., Difilippantonio, M.J., Wilson, P.C., Hanitsch, L., Celeste, A., Muramatsu, M., Pilch, D.R., et al. (2001). AID is required to initiate Nbs1/gamma-H2AX focus formation and mutations at sites of class switching. Nature *414*, 660–665.

Rappold, I., Iwabuchi, K., Date, T., and Chen, J. (2001). Tumor suppressor p53 binding protein 1 (53BP1) is involved in DNA damage-signaling pathways. J. Cell Biol. *153*, 613–620.

Rogakou, E.P., Pilch, D.R., Orr, A.H., Ivanova, V.S., and Bonner, W.M. (1998). DNA double-stranded breaks induce histone H2AX phosphorylation on serine 139. J. Biol. Chem. *273*, 5858–5868.

Rogakou, E.P., Boon, C., Redon, C., and Bonner, W.M. (1999). Megabase chromatin domains involved in DNA double-strand breaks in vivo. J. Cell Biol. *146*, 905–916.

Schaffner, C., Stilgenbauer, S., Rappold, G.A., Dohner, H., and Lichter, P. (1999). Somatic ATM mutations indicate a pathogenic role of ATM in B-cell chronic lymphocytic leukemia. Blood *94*, 748–753.

Schultz, L.B., Chehab, N.H., Malikzay, A., and Halazonetis, T.D. (2000). p53 binding protein 1 (53BP1) is an early participant in the cellular response to DNA double-strand breaks. J. Cell Biol. *151*, 1381–1390.

Sleckman, B.P., Bardon, C.G., Ferrini, R., Davidson, L., and Alt, F.W. (1997). Function of the TCRα enhancer in αβ and γδ T cells. Immunity *7*, 505–515.

Smogorzewska, A., Karlseder, J., Holtgreve-Grez, H., Jauch, A., and de Lange, T. (2002). DNA ligase IV-dependent NHEJ of deprotected mammalian telomeres in G1 and G2. Curr. Biol. *12*, 1635–1644.

Stewart, G.S., Wang, B., Bignell, C.R., Taylor, A.M., and Elledge, S.J. (2003). MDC1 is a mediator of the mammalian DNA damage checkpoint. Nature *421*, 961–966.

Stilgenbauer, S., Winkler, D., Ott, G., Schaffner, C., Leopolt, E., Bentz, M., Moller, P., Muller-Hermelink, H.K., James, M.R., Lichter, P., and Dohner, H. (1999). Molecular characterization of 11q deletions points to a pathogenic role of the ATM gene in mantle cell lymphoma. Blood *94*, 3262–3264.

Vogelstein, B., Lane, D., and Levine, A.J. (2000). Surfing the p53 network. Nature *408*, 307–310.

Wang, B., Matsuoka, S., Carpenter, P.B., and Elledge, S.J. (2002). 53BP1, a mediator of the DNA damage checkpoint. Science *298*, 1435–1438.

Ward, I.M., and Chen, J. (2001). Histone H2AX is phosphorylated in an ATR-dependent manner in response to replicational stress. J. Biol. Chem. *276*, 47759–47762.

Ward, I.M., Minn, K., van Deursen, J., and Chen, J. (2003). p53 binding protein 53BP1 is required for DNA damage responses and tumor suppression in mice. Mol. Cell. Biol. *23*, 2556–2563.

Zhu, C., Mills, K.D., Ferguson, D.O., Lee, C., Manis, J., Fleming, J., Gao, Y., Morton, C.C., and Alt, F.W. (2002). Unrepaired DNA breaks in p53-deficient cells lead to oncogenic gene amplification subsequent to translocations. Cell *109*, 811–821.